High-resolution impedance spectroscopy: application to the study of semiconductor devices and estimating of their efficiency for application in bioelectronics

© N.A. Boitsova,[1] A.A. Abelit,[1] N.A. Verlov,[2] D.D. Stupin[1]

[1]Alferov University,
194021 Saint Petersburg, Russia
[2]St. Petersburg Nuclear Physics Institute, National Research Center Kurchatov Institute,
188300 Gatchina, Russia
e-mail: natab2002@yandex.ru

Received May 5, 2025
Revised June 23, 2025
Accepted June 30, 2025

The reliability and accuracy of comparing experimentally observed phenomena with theoretical concepts always increases with the amount of useful experimental information. In this paper, we demonstrated the advantages of using high-resolution impedance spectroscopy (HRIS) for diagnostics of semiconductor devices. We demonstrated that HRIS not only allows one to obtain the classical capacitance-voltage (CV) characteristics of semiconductor devices but also to recognize the nature of their electrical properties, in particular, to detect leakage in $p-n$ junctions. Furthermore, through subsequent comparative analysis of HRIS data for semiconductor devices and bioelectrodes, we found that their spectra are generally well described by R-CPE circuits, which can be used in the design of bioelectronic devices using both metal and semiconductor electrodes.

Keywords: equivalent circuits, high-resolution spectra, impedance spectroscopy, complex non-linear least squares, photodiode, solar cell, bioelectrodes.

DOI: 10.61011/TP.2025.12.62375.240-25

Introduction

Almost just after its emerging in 1886 [1] electrical impedance spectroscopy, which is a powerful future-proof technique for investigation of samples of the most diverse nature, faced the nessesarity for creating algorithms for processing experimental data. This problem was especially evident after studies by Warburg and Cole-Cole [1,2], which found a phenomenon of capacitance dispersion (or a pseudo-capacitance effect) when investigating chemical and biological samples [1,2]. A universal and available solution of the impedance-spectra processing appeared only recently, in the 1990-s, in the studies by J. Ross Macdonald, who created a DOS-application LEVM for processing impedance spectra by means of a complex non-linear least-square method (CNLS) [3]. Several commercial and free LEVM analogs have appeared for the last 25 years, but these software products are either supplied as closed-source applications, thereby significantly complicating their application for challenging scientific purposes, or as open-source applications, which are outdated or neglect the latest computer engineering achievements. In particular, the software programs LEVM [3], Zview [4] and EC-Lab [5] neither support high-resolution spectra processing nor provide it correctly [6].

In order to overcome the these problems on the way of improving the impedance-spectra processing methods, we created the MatLab/GNU Octave software NELM [6] based on CNLS application for searching equivalent schemes. Our software support of the high-resolution spectra processing (the highly-informative spectra) and use of a parallel computation technique for accelerating their calculations [7]. Despite of the software NELM was initially created for processing the biological data, it is a universal tool and suitable for approximating of the impedance spectra (IS) of the wide range of the samples, including the semiconductor devices, which is demonstrated in the present study. During its course, we set the goal to show advantages of application of HRIS and CNLS for studying properties of the photodiodes and the solar cells. Additionally, we also clearly showed common features and differences between the impedance spectra of the semiconductor devices and bioelectrodes. The data obtained as a result of this comparison can be used for designing and optimizing bioelectronic sensors, in particular, when developing their software and when selecting materials for manufacturing their electrodes.

1. Materials and methods

The biological impedance spectra are often analyzed using a RL-CPE circuit, whose special case of a RC-circuit is an equivalent scheme for the $p-n$-junction [1]. For this reason, we choose the models for CNLS approximation as circuits that consisted of CPE-elements (constant phase elements) and resistors (inductance was taken into account as a spurious element [7]). Note that impedance of the CPE-element is defined by the formula $Z = 1/[W \cdot (i\omega)^{\alpha}] = 1/[C(\omega) \cdot i\omega]$,

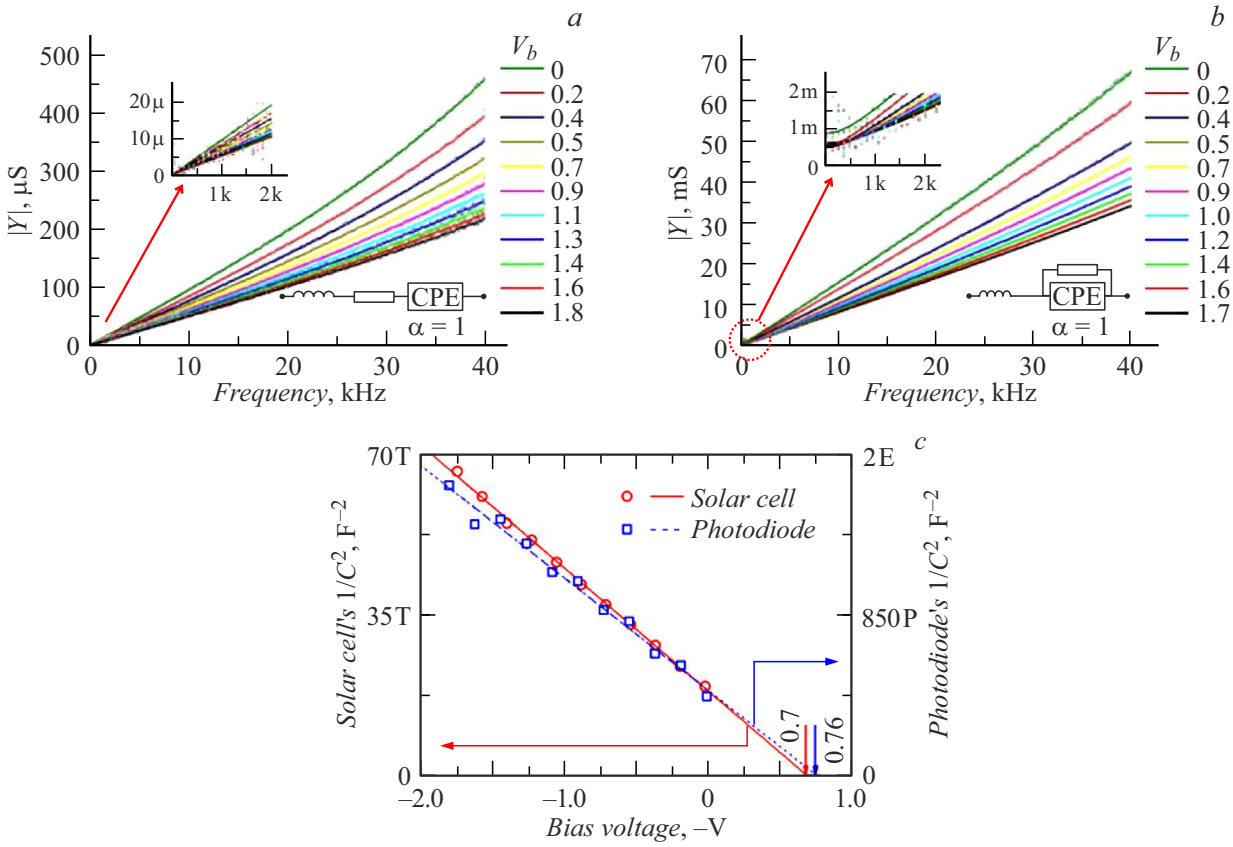

Figure 1. Admittance spectra (Y) for the photodiode BPW 20 RF (a) and the solar cell DSM (b) and their CV-characteristics (c). The dots mark experimental data (the spectra are decimated for clarity of the graphs), while the solid lines mark approximations. It can be seen that for both the devices conductivity decreases with an increase of reverse-bias voltage amplitude due to extending of a space charge region. A linear form of the CV-curves in a representation „voltage *v.s.* $1/C^2$" indicates that the $p-n$-junctions in these devices are abrupt, while their diffusion potential is about 0.7–0.76 V. Differences in the back-biase Vb values in the panels a and b are related to specific features of operation of a digital-to-analog converter, which was used as a controllable source of DC voltage supplied to the semiconductor devices.

where α is a CPE-exponent, W is pseudo-capacitance, $C(\omega) = W \cdot (i\omega)^{\alpha-1}$ is a function that describes a frequency dependence of capacitance (its dispersion), and ω is a frequency. Nowadays, no unique explanation for a nature of the capacitance dispersion phenomenon, but its presence in the impedance spectra can indicate the presence of pores and defects or strong diffusion effects in the studied system [1]. Our samples included a silicon photodiode BPW 20 RF (Vishay, USA), a silicon solar cell DSM (Dobraya Energia, Russia), a TiN-electrode from a commercial multi-electrode matrix 60StimMEA200/30-Ti (MultiChannels Systems, Germany) as well as a Sn electrode manufactured in an SPbAU Bioelectronics laboratory. The impedance spectra were measured in a frequency range from 10 Hz to 40 kHz with resolution of 2 Hz and a excitation voltage amplitude of 15 mV using an setup described in the studies [1,8] by the Fourier-EIS method [1]. The bioelectrodes were studied in a 0.9 % NaCl solution. The characteristics of the semiconductor instruments were measured during their shading.

2. Results and discussion

The experimentally-obtained spectra as well as their CNLS approximations are shown in Fig. 1 and 2. The equivalent schemes used for analysis, which were selected for each sample by physical grounds (see Table) and mathematical statistics criteria (an approximation error shall be compared with a noise level), are shown in additional inserts. As it is clear from the provided data, unlike classical single-frequency approaches, application of the high-resolution spectra makes it possible to decompose the measured impedance spectra into a connection of two-terminal elements, wherein each of them describes certain region of the studied samples (see Table).

Moreover, during CNLS analysis of the obtained impedance spectra we found that in case of investigation of the photodiode and the solar cell their CPE-exponents α had turned out to be close to unity and independent of bias voltage. This observation agrees with the classical semiconductor theory [9] and means that the $p-n$-junctions in the studied semiconductor samples work as ideal capacitors.

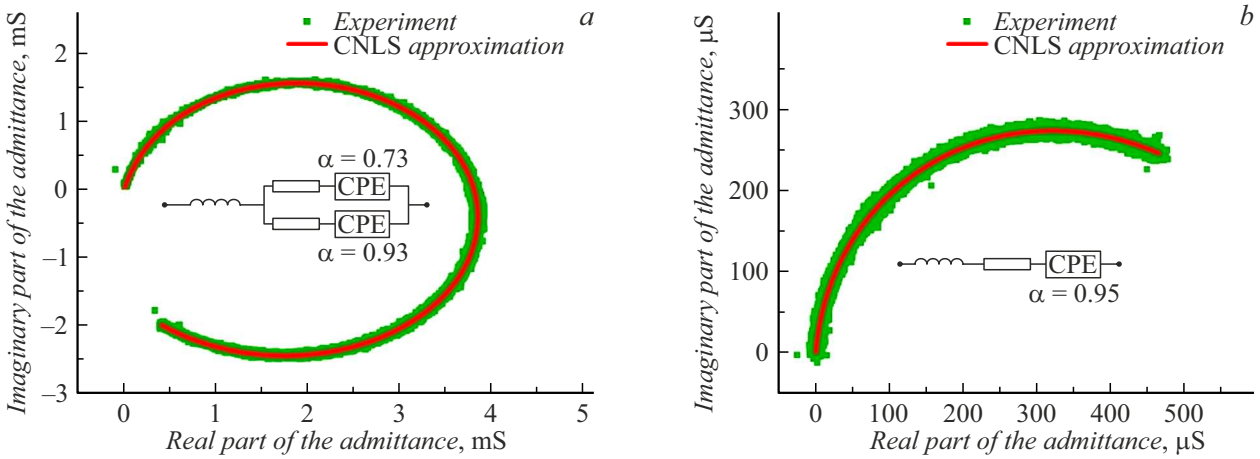

Figure 2. Admittance locuses for: *a* — the Sn electrode; *b* — the titanium nitride electrode. Here, CNLS means complex non-linear least squares (CNLS).

Comparison of elements of the equivalent circuit with physical/chemical phenomena in the semiconductors and the bioelectrodes [1]

Element	Semiconductors	Bioelectrodes
CPE-element	$p-n$-junction	Interface metal/electrolyte
Active resistance	Base resistance or resistance of leakage	Resistance of electrolyte and intercell space

It also follows from the obtained impedance spectra that the properties of the photodiode can be described by a series RC-circuit with a very low value $R < 100\,\Omega$. At the same time, it follows from Fig. 1, *b* that approximation of the impedance spectra of the solar cell requires to use a parallel RC-model with $R \sim 1\,\text{k}\Omega$, since its conductivity at the low frequencies is not zero (cf. the inserts in Fig. 1, *a* and *b*). This behavior of the impedance spectra indicates that unlike the photodiode, the structure of the solar cell has shunting defects. As a result of further analysis of the impedance spectra, we found that the CV-curves of both the semiconductor devices corresponded to a case of the abrupt $p-n$-junctions, while the diffusion potential value obtained therefrom is close to 0.7–0.76 V. For the photodiode BPW 20 RF, the similar diffusion potential value was obtained from a digitized CV-graph from its datasheet [10].

In case of investigation of the bioelectrodes, we found that unlike the semiconductor devices they are described by means of equivalent schemes that consist of the R-CPE circuits with $\alpha < 1$, i.e. of nonideal capacitors: in case of the TiN-electrode the spectrum is well described by one R-CPE circuit, while in case of the Sn-electrodes two parallel R-CPE-circuits are required to completely describe their electrical properties. It was also noted that the values of the CPE-exponents for both the electrodes were observed within the range 0.7–0.95.

Thus, it can be concluded from the obtained data that by means of CNLS HRIS allows multifacetedly diagnosing not only the semiconductor instruments, but the bioelectrodes as well, thereby indicating that a unified data processing algorithm can be used in the software device of impedance biosensors with replaceable metal and semiconductor electrodes.

Conclusions

The software NELM was used in the present study to demonstrate advantages of the high-resolution EIS for investigating the resistive-pseudo-capacitance samples, such as the $p-n$-junctions and the bioelectrodes. In particular, we have shown that approximation of the high-resolution spectra in case of investigation of the semiconductor samples makes it possible to highlight responses from the space charge region, series resistance and leakage resistance in their admittance signal. At the same time, experimentally-obtained identity of the equivalent schemes of the semiconductor samples and the bioelectrodes can be used for further combining of the semiconductor and bioelectronic technologies. We hope that the results of the study not only will be applied in the semiconductor industry, in which it is still relevant to create new diagnosis equipment [11,12], but open new horizons in biosensor engineering as well.

Acknowledgments

The authors would like to thank M.V. Dubina for providing the solar modules and for comprehensive assistance and support, and the authors also would like to thank A.V. Nashchekin and A.E. Zhukov for valuable discussions and pieces of advices.

Funding

The study was supported by the Ministry of Science and Higher Education of the Russian Federation (state assignment FSRM-2024-0001).

Conflict of interest

The authors declare that they have no conflict of interest.

References

[1] D.D. Stupin, E.A. Kuzina, A.A. Abelit, A.K. Emelyanov, D.M. Nikolaev, M.N. Ryazantsev, S.V. Koniakhin, M.V. Dubina. ACS Biomater. Sci. Eng., **7** (6), 1962 (2021). DOI: 10.1021/acsbiomaterials.0c01570
[2] E.T. McAdams, J. Jossinet. Physiolog. Measurement, **16** (3A), A1 (1995). DOI: 10.1088/0967-3334/16/3A/001
[3] J. Ross Macdonald, J. Schoonman, A.P. Lehnen. J. Electroanalytical Chem. Interfacial Electrochem., **131**, 77 (1982). DOI: 10.1016/0022-0728(82)87062-9
[4] D. Johnson. *ZView: A software program for IES analysis, Version 2.8* (Scribner Associates Inc., Southern Pines, NC, 2002), https://www.scribner.com/software/68-general-electrochemistr376-zview-for-windows/
[5] *BioLogic Science Instruments. EC-LAB Software: Techniques and Applications* (2011), https://mmrc.caltech.edu/BioLogic%20Echem/ECLab%20Manuals/EC-Lab%20software%20Techniques%20and%20Applications%20manual.pdf
[6] N.A. Boitsova, A.A. Abelit, D.D. Stupin. NELM: *Modern Open-Source Software for Multipurpose Impedance Spectra Analysis*. arXiv preprint arXiv:2506.01997 (2025), https://github.com/BioElectronicsLab/NELM-1.0-beta
[7] N.A. Boitsova, A.A. Abelit, A.N. Verlov, D.D. Stupin. St. Petersburg Polytechnic Univer. J.: Phys. Mathem., **75** (3.1), 315 (2024).
[8] D.D. Stupin, S.V. Koniakhin, N.A. Verlov, M.V. Dubina. Phys. Rev. Appl., **7**, 5 (2017). DOI: 10.1103/PhysRevApplied.7.054024
[9] S.M. Sze. *Fysics of Semiconductor Devices* (John Wiley & Sons, NY., 1969), DOI: 10.1002/04700683P29
[10] *Vishay Semiconductors, BPW20RF manual* (Fig. 6, Rev. 1, 19-Mar-02), https://www.vishay.com/docs/81570/bpw20rf.pdf
[11] G. Yakovlev, V. Zubkov, A. Solomnikova, O. Derevianko. Turk. J. Phys., **42** (4), 433 (2018). DOI: 10.3906/fiz-1803-23
[12] D.V. Mokhov, T.N. Berezovskaya, A.G. Kuzmenkov, N.A. Maleev, S.N. Timoshnev, V.M. Ustinov. Tech. Phys. Lett., **43**, 909 (2017). DOI: 10.1134/S1063785017100091

Translated by M.Shevelev